METHODS AND ANALYSIS OF THE RELIABILITY PARAMETERS FOR DRIVER GROUPS AND STATIONS FOR BELT CONVEYORS

Petko Nedyalkov

University of Mining and Geology “St. Ivan Rilski” - Sofia, Faculty of Mining Electromechanics, E-mail, petko.nedyalkov@mgu.bg

ABSTRACT: The presented study surveys the methods for analysis, estimation, and technical application of procedures for the systematisation and check of the reliability indicators of the driver groups and stations in heavy loaded mining belt conveyors. The base indicators influencing over the reliability are the loading and the maintenance and both of them are subjected to a statistical assessment. Some of the particular factors that are the subjects of the methods are investigated in depth. The major cases of analysis through modelling of the drive - force – load mechanical system interaction are examined. Basic force, torque, and power dependences between the structural assemblies in the driver group and station for the belt conveyor are also examined. Dynamic models for the diver - mechanical system are created and analysed. Indicative results are presented in the form of diagrams and tables, which are subject to estimation and comparative analysis to the load in a real technological system.

KEYWORDS: *belt conveyor, reliability, force analysis, dynamical analysis.*

МЕТОДИКА И АНАЛИЗ НА НАДЕЖДНОСТТА НА ЗАДВИЖВАЩИТЕ ГРУПИ И СТАНЦИИ ЗА ГУМЕНО-ЛЕНТОВИ ТРАНСПОРТЬОРИ

Петко Недялков

Минно–геоложки университет „Св. Иван Рилски“ – София, Минноелектромеханичен факултет

РЕЗЮМЕ: В работата се дава обзор на методика за анализ, оценка и техническа изпълнимост на процедури за систематизиране и проверка на показателите на надеждността за задвижващи групи и станции за тежконатоварени гумено-лентови транспортьори в условията на минните предприятия. Основните фактори, влияещи върху надеждността, са натоварване и поддръжка, като и двата фактора могат да се оценят и статистически. Част от показателите субекти на методиката са разгледани задълбочено за отделни частни случаи. Разгледани са основните случаи на моделиране и анализ на натоварването на механичната система. Разгледани са основните силови, моментови и мощностни зависимости между възлите в задвижващата станция на гумено-лентов транспортьор. Създадени са и са анализирани динамични модели на механичната система, представени са индикативни резултати в графичен и табличен вид, като резултатите служат за оценка и сравнителен анализ с натоварването в производствената система.

КЛЮЧОВИ ДУМИ: *гумено-лентов транспортьор, надеждност, силов анализ, динамичен анализ*

INTRODUCTION

Rubber belt conveyors /RBCs/ are machines for continuous transport in the entire main and supporting range of mining and extracting activities for coal, ore minerals, inert earth-rock materials, overburden, industrial waste, and ash residues from filters and heat plants. RBCs are experiencing a "renaissance" in modern technological schemes with the possibility of shortening of the transport-conveyance distance of mining trucks by installing inclined conveyors through the inmobile board of the mine or through inclined transport fabrication, which can shorten the truck travel by up to 5 times (Shamsi 2021). Belt conveyors are the main means of transport for all activities in this type of mining technological scheme, so the importance of reliability parameters increases.

RBCs designed as shown at the scheme in Fig. 2 are preferred in mining and ore processing plants - with two drive drums onto which two or three drive groups can be installed, depending on the location of the specific conveyor in the technological scheme of the mine.

As high-performance machines, the reliability performance of RBCs is formed by numerous indicators, with current development focusing on driving stations and groupsets. Considering various highly loaded RB conveyors installed and used in mines of *Asarel*, *Troyanovo-Sever*, *Troyanovo-1*, and *Troyanovo-3*, it should be noted the installed high power capacity: 2 to 3 MW per drive station for a continuous production cycle at planned preventive maintenance /PM/ times - for maintenance work up to 2 hours a day and planned annual repairs up to 20 days a year.

With these indicators, all repair activities should be carried out according to a scheme of replacement of nodes in order to reduce the time of the maintenance. The use of identical conveyors is preferred for the purpose of unit unification under production conditions, but with the possibility of reconfiguration to ensure the readiness of the conveyor for the particular task or stopes.

THEORY AND METHODOLOGY

The study is based on the following methodology:

- general analysis of reliability indicators;
- analysis of bearings, as elements ensuring movement;
- analysis of rotating nodes, as subject to balance/imbalance;
- analysis of structural elements and metal structures in order to establish loss of stability;
- dynamic analysis of the driver system for calculation and evaluation of resonance areas, shown by the block diagram in Fig. 1.

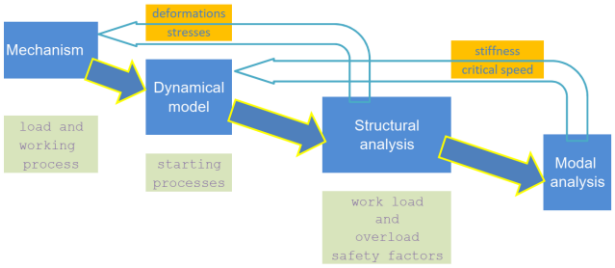

Fig. 1. Block diagram of dependencies in dynamic mechanical system modelling

The main parameters affecting the durability of the units in the driver group and station of the rubber belt conveyor are the accidental overloads (Lazov 2018, Lazov 2018, Bortnowski 2021, Bortnowski 2022) in the range between 1.1 to 1.3 times of the nominal, counting that the thermal protections of the drive motors would shut down in an emergency at overload from 1.3 to 1.5 of the nominal.

Reliability parameters

In these ranges, force and moment overload should not cause damage or drastic destruction of a part or a node. In this setup, the following causes can be distinguished from the known causes of damage: fatigue, resonance, random (stochastic) overload, and imbalances in balancing the resulting inertial overload.

With generalised parameters of reliability, the following values can be defined for the operation (time) without damage /TOT/:

- target operation time – $TOT_{t\text{-}1}$ = 50E3 h;
- reasonable operation time – $TOT_{r\text{-}2}$ = 20E3 h;
- net working time per year – $TOT_{A\text{-}Y3}$ = 7500 h.

At a reported average time to failure for any of the nodes listed above – MTTF = 8500 h, the parameters are calculated as follows:

- intensity of failures – $IF = TOT_i/MTTF$;
- failure rate assuming an exponential distribution of the failure and survival function: $FR_i = I = IF/TOT_i$
- survival function: $S(t) = \exp(-I*t)$

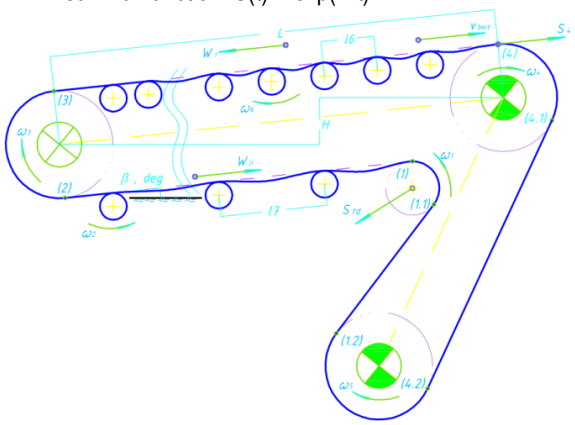

Fig. 2. Scheme of a RBC with the main elements

Table 1. *Calculated reliability parameters*

$TOT_{a\text{-}y3}$	7550	h		
$TOT_{t\text{-}1}$	50000	h		
$TOT_{t\text{-}r\text{-}2}$	20000	h		
$MTTF=TOT_{t\text{-}r\text{-}3}$	8500	h		
z =	1	3	15	
IF_1	0.151	0.5	2.3	
IF_2	0.378	1.1	5.7	
IF_3	0.888	2.7	13.3	
$I_1 = FR_1$	2.00E-05	6.0E-05	3.0E-04	
$I_2 = FR_2$	5.00E-05	1.5E-04	7.5E-04	
$I_3 = FR_3$	1.18E-04	3.5E-04	1.8E-03	
	S(t, z=1)	S(t, z=3)	S(t, z=15)	t, h
$S_1(t,z),\%$	86.07	63.76	10.54	7500
$S_1(t,z),\%$	74.08	40.66	1.11	15000
$S_1(t,z),\%$	63.76	25.92	0.12	22500

The results for the reliability parameters are shown in Table. 1 for different number of driver groups z. The different number of driver groups is determined by the location and inclination of the RBC in the general mine transport scheme.

With the values set in this way, it could be seen from Table 1 that with an average reported survival time MTTF=8500 h, the survival function calculated for net operation time per one year (t=7500 h) for 15 groups (z=15) is 10%, or in other words - repair dead time should be planned to replace a group at about 784 working hours.

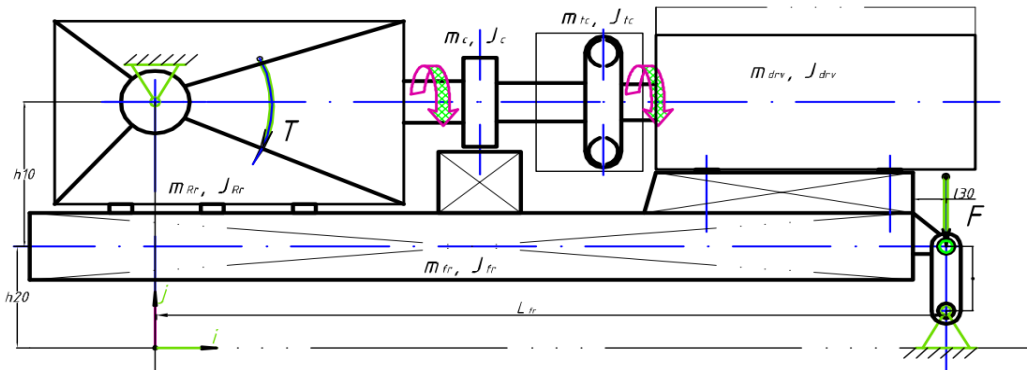

Fig. 3. Block diagram of the driver group

Load and life-cycle of bearings

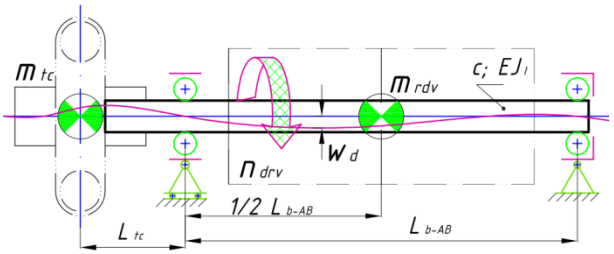

Fig. 4. Electric motor shaft with suspended masses

Figure 3 shows the block diagram of the driver group and Figure 4 - the scheme for loading and supports of the shaft of the electric motor. According to these schemes, the indicators of the nodes, drive, and suspension, as well as the indicators of the bearings are calculated. The scheme in Figure 3 presents the kinematic drive chain, namely: engine – hydrodynamic clutch – clutch/brake – reducer – drive drum. The suspension of the reducers and the drive drum is the same, namely the drive drum bearings, the reactive forces from the drive drum are transmitted through the reducer housing and frame to the reaction rod.

Table 2. *Calculation indicators of the bearings of the considered electric motor* (Nedyalkov 2008; SKF 2023)

	d	D	B	C	C_0	F_{LR}	$e = k_{AL}$
	mm	mm	mm	kN	kN	kN	
NU 328 ECM	140	300	62	780	830	10	0
				X	1	15	
n	1370	rpm		Y	0	20	
a	3.33					30	
6328 C3	140	300	62	251	245	2.92	
X	0.46			X	1	4.39	0.54
Y	1.71	f_0		14 Y	0	5.85	
a	3					8.77	

F_{LA}	$f_0 \cdot F_{LA}/C_0$	P	C/P	L_{10}	L_{10h}	$L_{10h}/50k$
kN		kN		10^6 rpm	h	
0		10.0	78	474552	5773139	115.5
0		15.0	52	140608	1710560	34.2
0		20.0	39	59319	721642	14.4
0		30.0	26	17576	213820	4.3
1.59	0.09	4.1	61.8	236447	2876484	57.5
2.38	0.14	6.1	41.2	70058	852292	17.0
3.17	0.18	8.1	30.9	29556	359561	7.2
4.76	0.27	12.2	20.6	8757	106536	2.1

At an established mode of operation with a constant load, the bearings of all equipment are calculated for a life of 20 to 50 thousand hours, as the last column of Table 2 presents a result for the example calculation of a 630 kW, 6 kV, 1370 rpm, 450L motor for the ratio of the calculated bearing life to 50 thousand hours (L10h/50*10E3), at different support reactions. This ratio guarantees a safety coefficient for bearing life with ranges over the limit of 50,000 hours. It could be seen that for both bearings of the electric motor, the values of this coefficient significantly exceed one. The different support reactions for the same rotor are determined by the different clutches or belt drives mounted on the motor shaft.

The results in Table 2 show that even in the most severe load case presented in row 8, both motor bearings have a life twice the limit of 50,000 hours. The frequency calculation of the considered bearings for a fixed mode is presented in Table 3, and these results also do not show an intersection of the frequency characteristics of the bearings with those of the rotor of the electric motor.

Table 3. *Frequency calculation of electric motor bearings* (Nedyalkov 2008; SKF 2023)

	d_p	d_r	z_r	n_s
	mm	mm		rpm
NU 328 ECM	222	42	14	1380
6328 C3	220	47.625	8	1380

f_s	f_i	f_o	f_c	f_b	f_r
SF	**BPFI**	**BPFO**	**FTF**	**BSF**	**REDF**
Hz	Hz	Hz	Hz	Hz	Hz
23.0	191.5	130.5	9.3	58.6	117.2
23.0	111.9	72.1	9.0	50.6	101.3

CPM_s	CPM_i	CPM_o	CPM_c	CPM_b	CPM_r
SF	**BPFI**	**BPFO**	**FTF**	**BSF**	**REDF**
rpm	rpm	rpm	rpm	rpm	rpm
1380.0	11487.5	7832.5	559.4	3516.6	7033.2
1380.0	6715.0	4325.0	540.7	3038.0	6076.1

Mechanism and dynamic model

The driver system for the first step of idealisation can be idealised to the model shown in Fig. 5. A model shown (OSMC 2023, SimX 2023) in this figure was synthesised and developed in order to study the starting and braking processes in the conveyor through a single-mass model with variable load parameters. The model allows changing both the type and form of resistances and the type and form of starting and braking procedures. The main purpose of the presented model is to allow the study of atypical combinations in the load cases of the driver electric motor, as well as different characteristics of the starting process.

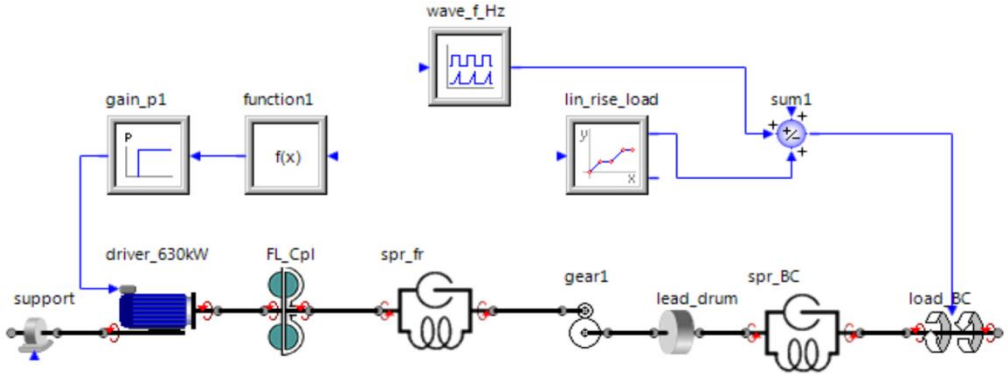

Fig. 5. Dynamic model of the driver group

The starting processes in transporters are a serious research topic (Lodijewiks 2006, Daijie He 2016) for industrial research because of the idealizations and restriction from the laboratory equipment. The type of starting and braking processes determine the length of the start and the average load during the starting procedure (Harrison 1986, Harrison 1983, Gladysiewicz 2019). Figure 6 shows the power, torque, and angular velocity results of the electric motor for starting process using a start-up procedure for belt stresses lightening (Nuttall, 2007).

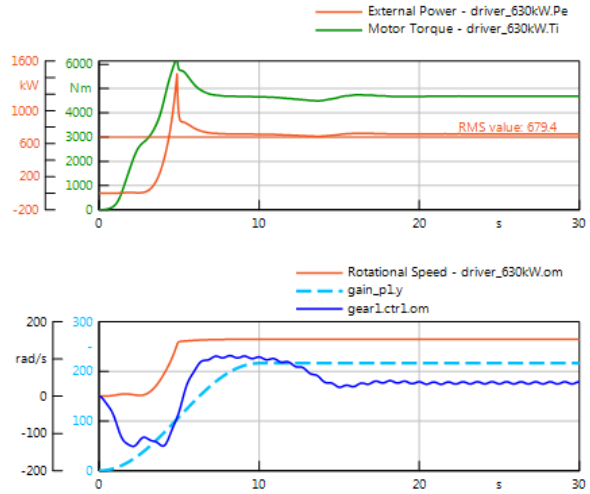

Fig. 6. Example diagram of electric motor parameters for the starting process

The simplified start-up procedure of belt conveyors (Nuttall 2007) uses a dependency of the following type:

$$i_{start} = I_n \cdot \frac{k_I}{2} \cdot \left[1 - \cos\left(\frac{\pi \cdot t}{t_{start}}\right)\right], A$$

where:

I_n is the nominal current of the electric motor;

k_I is the start-up coefficient as foe current for the electric motor;

t_{start} is the time for starting.

Figure 6 presents the motor performance from a simulation for a starting duration of 10s, showing an average starting power of 680 kW. It can be seen that there is no overload for all the modeled processes.

Critical speed of the motor shaft

The balancing of all machines for industrial use goes through several stages, and the permissible static balance of the corresponding rotating part is indicated in the passport data of the machine. Also, for most machines, passport data is available for the permissible misalignment during installation and operation. A resulting parameter from these two indicators is the vibration load of the mounted machine unit, whose measurable indicator is the permissible vibration speed or vibration acceleration of the housing or other main part. This measurable indicator is significantly influenced by the state of bearing units (Nedyalkov 2008; SKF 2023), and systems for continuous control of machine and unit indicators very often use a signal from such type of sensors to track wear or damage in bearings and associated nodes. A system of this type operates with multiple points by traversing and recording the signal from the various points and providing a signal or report to the dispatcher.

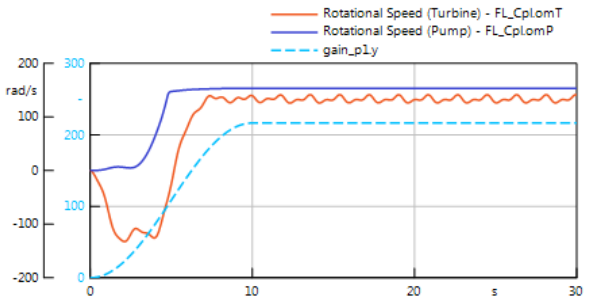

Fig. 7. Example diagram of the turbo clutch indicators for the start-up process

While the static balancing as described above is a relatively well-defined process and industrial procedures are available to manage the performance of machines depending on it, in dynamic balancing of rotating nodes and machines things are not so well set (IEC 60034- 1). Critical rpm of rotating shafts are the subject of serious research and development in turbine machines, internal combustion engines, etc., but in standard unified medium-speed machines (up to 3000 rpm) such information is missing. Example: electric motor catalogues do not list [OMEC 2023, Helmke 2023] rotor weight data, only its mass moment of inertia. Data are given for the bearings, and the permissible force on the motor shaft in terms of belt or chain gear tension, but no data are given for the permissible mass of the clutch with the corresponding assembly.

The effects in the presence of bending oscillations of the motor shaft with their corresponding critical rpm are one of the few deterministic approaches to elucidate a correlation between a rotating rotor and a change in bearing responses during that rotation.

The idealised scheme of critical rpm calculation gives the ratio:

$$\omega_{0i} = \sqrt{\frac{c_{sh}}{m_{i-disk}}}, rad/s,$$

where:

c_{sh} is the stiffness of the shaft for the corresponding section

$m_{i\text{-}disk}$ is the mass of the corresponding disk.

In this computation model, it is assumed that only the shaft is deformed, and all other details, including the bearings, are non-deformable. The stiffness of the shaft is calculated by various methods and calculation systems, while most often the mass is known. For a console part of the shaft, a centrally loaded shaft with a distributed load and a concentrated force, the dependencies are known:

$$c_{con} = \frac{3 \cdot E_y \cdot J_A}{L_i^3}, N/m$$

$$c_{bq} = \frac{384 \cdot E_y \cdot J_A}{5 \cdot L_i^3}, N/m$$

$$c_{cF} = \frac{48 \cdot E_y \cdot J_A}{L_i^3}, N/m,$$

where:

E_y is the modulus of elasticity of the shaft material,

J_A is the moment of inertia of the shaft section,

L_i is the length of the corresponding section,

c_{con} – is console part stiffness,
c_{bq} – is distributed load stiffness,
c_{cF} – is stiffness corresponding to concentrated load.
On the other hand, shaft stiffness can be calculated by:

$$c = F_i/w_{st}\ , N/m\ ,$$

where w_{st} is the static sag under the force F_i. This dependence allows the connection of deformations in the shaft with its critical revolutions.

When experimentally measuring the critical rpm of the shafts, it is considered that the above dependences are estimated, in other words, there is a deviation between the measured value and the calculated value. It is accepted that the critical rpm for real machines are estimated as a critical area with a range of about 80 to 120% of the calculated critical angular speed. Dependencies for evaluating the mutual influence of several critical masses also give a deviation from the measured value, and the Dunkerley or Rayleigh methods can be used.

$$\omega_{0-Dunkerley} \cong \sqrt{\frac{1}{\omega_1^2}+\frac{1}{\omega_2^2}+\ldots+\frac{1}{\omega_i^2}}, rad/s$$

$$\omega_{0-Rayleigh} \cong \sqrt{\frac{g\cdot\sum G_i\cdot w_i}{\sum G_i\cdot w_i^2}}, cycles/s$$

These calculations were carried out for the selected engine and clutch and the results are given in Table 4. Since the formulae above are estimated (approximate), they allow the interpretation of at least two cases of loading and deformations in the shaft. The first case assumes the stiffness of the shaft as maximum possible; in other words, the rotor stiffens the shaft, which fits into the requirements of standard IEC 60034-1. The second case assumes the stiffness of the shaft according to its section.

Table 4. *Frequency calculation of shaft – rotor system*

	n_n, rad/s| Hz| rpm			145	23	1380
	m_i	$w_{i\text{-}ст}$	c_i	$\omega_{0\text{-}i}$	$f_{0\text{-}i}$	
	kg	mm	kN/mm	rad/s	Hz	rpm
shaft	229	0.1352	17.7	277.7	44.2	2652
rotor (shaft stf)	1637	0.1352	17.7	104.0	16.5	993
rotor	1637	0.0002	70.8	207.9	33.1	1985
Turbo coupling	650	0.0112	604.6	964.5	153.5	9210
			Rayleigh	190.4	30.3	1819
case - stiff			Dunkerley	203.2	32.3	1941
			Rayleigh	54.3	8.6	519
case - soft			Dunkerley	103.4	16.4	987

The second case corresponds to a double (or repeatedly) bent elastic line of the shaft, when the entire load is transmitted only through the shaft. The assessment of critical rpm and areas is presented in the last row of the Table. 4, both values being below the engine's rated operating speed. The Rayleigh estimate is expectedly very low (47% lower), and the Dunkerley estimate is 0.58% - the lowest frequency for a single mass on the shaft. Dunkerley's formula estimate is 71.5% of the rated engine rpm. At critical revolutions, the bearing load cannot be calculated with the formulae from the previous section. The dynamic force on the bearing is:

$$F_{dyn-b} = c_b \cdot w_d,$$

Which, for a deformation of about 150um (as much as the standardised clearance in the bearing) for the considered case, corresponds to ~6 kN force in the axial direction. This force is enough to drop the bearing's durability from 50,000 hours to 20,000 hours.

Conclusions

The presented methodology and computing models make it possible to evaluate the influence between a driver system with a rotating load (torque) and the power load on the bearings of the electric motor by considering the effects of bending vibrations in the shaft. The dynamic model allows to perform a simulation with an overload of the system, the action of which overload is about 10 s, and the angular speed of rotation of the turbine wheel of the hydrodynamic clutch is in the critical zone calculated in Table 4.

In order to upgrade and improve the methodology, it is necessary to develop a research model for the modal study of the electric motor shaft and the masses attached to it using the Finite Element Method. With precise three-dimensional modelling, setting the correct characteristics of the materials, the position of the masses, and, particularly important, the correct support connections and reactions, the accuracy of the method can reach 2.5%, which for a similar task is an excellent result.

The future development of the methodology necessarily includes recording of experimental data, as the real system has more than two fixed masses to the shaft of the electric motor.

The effects of critical rpm on electric motors are not well represented at the cataloguing and standardisation level. In the catalogues, the maximum level of information includes the dimensions and type of bearings of the electric motor and tabulated values of the permissible forces acting on the motor shaft for installation reasons, which is not sufficient for the correct calculation and evaluation of the effects of the critical revolutions on the rotor. In order to evaluate the effects of bending oscillations on the electromagnetic force created by the rotor and the electromagnetic imbalance in a completeness sufficient for engineering practice, additional information is needed to parametrise a model including mechanical and electromagnetic interactions.

Acknowledgment. This research was supported by the MEMF 171/2022 internal regulation project of UMG “St. Ivan Rilski”.

References

Bortnowski, P., L. Gładysiewicz, R. Krol, M. Ozdoba. 2021. Models of Transverse Vibration in Conveyor Belt—Investigation and Analysis, ISSN:1996-1073, *Energies 14* (14) (2021) 4153, https://doi.org/10.3390/en14144153.

Bortnowski, P., W. Kawalec, R. Krol, M. Ozdoba. 2022. Identification of conveyor belt tension with the use of its transverse vibration frequencies, ISSN: 0263-2241, *Measurement 190* (2022), 110706, https://doi.org/10.1016/j.measurement.2022.110706

Daijie He, Pang Yusong, G. Lodewijks. 2016. Speed control of belt conveyors during transient operation, ISSN: 0032-5910,

Powder Technology 301 (2016) 622–631, http://dx.doi.org/10.1016/j.powtec.2016.07.004.

Gładysiewiczq L., R. Król, W. Kisielewski. 2019. Measurements of loads on belt conveyor idlers operated in real conditions, ISSN: 0263-2241, *Measurement 134* (2019) 336–344, https://doi.org/10.1016/j.measurement.2018.10.068.

Harrison, A. 1983. Criteria for minimising transient stress in conveyor. *Trans. Inst. Eng., Australian Mech. Eng.* 1983, ME8, 129–134, Australia.

Harrison, A. 1986. Determination of the natural frequencies of transverse vibration for conveyor belts with orthotropic properties, ISSN:1095-8568, *J. Sound Vib. 110* (3) (1986) 483–493, https://doi.org/10.1016/S0022-460X(86)80149-3

HELMKE. 2023. *High-Voltage Motors with Flameproof Enclosure*, helmke.de (visited 05.2023).

HOU You-fu, MENG Qing-rui. 2008. Dynamic characteristics of conveyor belts. ISSN: 1674-5264, *J China Univ Mining & Technol 18* (2008) pp. 629–633.

Lazov, L., N. Kotzev. 2014. Concerning on the choice of the crosssection of the main girder of bridge cranes, ISSN:0861-9727, *Mechanika na machinite*, 107, year 22, book 3, pp. 72-76, Varna (in Bulgarian with English abstract).

Lazov L., N. Kotzev, Kr. Krastanov. 2018. Mashini za neprekasnat transport, ISBN:978-954-12-0251-7*, VTU “T. Kableshkov”*, Sofia. (in Bulgarian)

Lodewijks, G. 1996. *Dynamics of Belt Systems* (dissertation thesis), ISBN: 90-370-145-9, TU Delft.

Nedyalkov, P., Dr. Vrazhilski, D. Ralev. 2008. Research over frequency band in roller bearing assembly at working conditions. ISSN: 1312–1820, *Annual of University of Mining and Geology, Vol. 51, book III*, pp. 79-82, UMG, Sofia. (in Bulgarian with English abstract).

Nuttall, Ash. 2007. *Design Aspects of Multiple Driven Belt Conveyors (dissertation thesis)*, ISBN 978-90-5584-092-2, TRAIL Research School, Delft, The Netherlands.

OMEC 2023. *OMEC motors, ELECTRIC MOTORS CATALOGUE*, omecmotors.com (visited 05.2023).

Open Source Modelica Consortium (OSMC 2023), OpenModelica, www.openmodelica.org (visited 05.2023)

Shamsi M., M. Nehring. 2021. Determination of the optimal transition point between a truck and shovel system and a semi-mobile in-pit crushing and conveying system, *Journal of the Southern African Institute of Mining and Metallurgy*, ISSN:2225-6253, vol. 121, no. 9, pp. 497–504, http://dx.doi.org/10.17159/2411- 9717/1564/2021.

SimulationX (SimX 2023), ESI Group, http://www.simulationx.com (vis. 05.2023)

SKF 2023. SKF.com, skf.bearingselect.com, (visited 05.2023)